Stoichiometry and Topology of the Complex of the Endogenous ATP Synthase Inhibitor Protein IF1 with Calmodulin

ARTICLE *in* BIOCHEMISTRY · SEPTEMBER 2010

Impact Factor: 3.02 · DOI: 10.1021/bi100447t · Source: PubMed

7 AUTHORS, INCLUDING:

Daniela Pagnozzi
Porto Conte Ricerche
62 PUBLICATIONS **814** CITATIONS
SEE PROFILE

Leila Birolo
University of Naples Federico II
46 PUBLICATIONS **612** CITATIONS
SEE PROFILE

Giovanna Lippe
University of Udine
41 PUBLICATIONS **788** CITATIONS
SEE PROFILE

Irene Mavelli
University of Udine
96 PUBLICATIONS **1,436** CITATIONS
SEE PROFILE

7542 *Biochemistry* **2010,** *49,* 7542–7552
DOI: 10.1021/bi100447t

BIOCHEMISTRY
including biophysical chemistry & molecular biology
Article

Stoichiometry and Topology of the Complex of the Endogenous ATP Synthase Inhibitor Protein IF_1 with Calmodulin[†]

Daniela Pagnozzi,[‡,▽] Leila Birolo,*[,‡,§] Gabriella Leo,[‡] Stefania Contessi,[⊥] Giovanna Lippe,[#] Pietro Pucci,[‡,∥] and Irene Mavelli[⊥]

[‡]*Department of Organic Chemistry and Biochemistry, and* [§]*School of Biotechnological Sciences, University of Napoli "Federico II", via Cynthia 6, 80126 Napoli, Italy,* [∥]*CEINGE-Biotecnologie Avanzate, Napoli, Italy,* [⊥]*Department of Biomedical Sciences and Technologies, MATI Centre of Excellence, University of Udine, Piazzale Kolbe 4, I-33100 Udine, Italy, and* [#]*Department of Food Science, University of Udine, via Sondrio 2/A, 33100 Udine, Italy.* [▽]*Present address: Porto Conte Ricerche Srl, Loc. Tramariglio, SP 55 Porto Conte/Capo Caccia Km 8.400, 07041 Alghero (SS), Italy.*

Received March 25, 2010; Revised Manuscript Received July 29, 2010

ABSTRACT: IF_1, the natural inhibitor protein of F_OF_1ATP synthase able to regulate the ATP hydrolytic activity of both mitochondrial and cell surface enzyme, exists in two oligomeric states depending on pH: an inactive, highly helical, tetrameric form above pH 6.7 and an active, inhibitory, dimeric form below pH 6.7 [Cabezon, E., Butler, P. J., Runswick, M. J., and Walker, J. E. (2000) *J. Biol. Chem. 275*, 25460−25464]. IF_1 is known to interact *in vitro* with the archetypal EF-hand calcium sensor calmodulin (CaM), as well to colocalize with CaM on the plasma membrane of cultured cells. Low resolution structural data were herein obtained in order to get insights into the molecular interaction between IF_1 and CaM. A combined structural proteomic strategy was used which integrates limited proteolysis and chemical cross-linking with mass spectrometric analysis. Specifically, chemical cross-linking data clearly indicate that the C-terminal lobe of CaM molecule contacts IF_1 within the inhibitory, flexible N-terminal region that is not involved in the dimeric interface in IF_1. Nevertheless, native mass spectrometry analysis demonstrated that in the micromolar range the stoichiometry of the IF_1−CaM complex is 1:1, thereby indicating that binding to CaM promotes IF_1 dimer dissociation without directly interfering with the intersubunit contacts of the IF_1 dimer. The relevance of the finding that only the C-terminal lobe of CaM is involved in the interaction is two fold: (i) the IF_1−CaM complex can be included in the category of noncanonical structures of CaM complexes; (ii) it can be inferred that the N-terminal region of CaM might have the opportunity to bind to a second target.

Bovine IF_1, the natural inhibitor protein of F_OF_1ATP synthase, consists of an 84 residue long monomer which folds into a single cationic amphiphilic α-helix (*1*). In solution, two IF_1 molecules dimerize by forming an antiparallel α-helical coiled-coil structure in the C-terminal region, leading the N-terminal regions to be available for binding to F_OF_1 (*1*) and other putative partners (*2*). The dimer is the predominant form at acidic pH, while at pH 6.5, it is in equilibrium with a tetrameric form which becomes predominant at basic pH (*3*).

Pedersen and Carafoli groups had previously reported that IF_1 is a target for Calmodulin (CaM[1]) (*4*, *5*), the archetypal EF-hand calcium sensor (*6*−*9*). CaM interacts and regulates numerous target proteins that are structurally and functionally unrelated, including metabolic enzymes, structural proteins, transcription factors, ion channels, and pumps, and modulates a wide range of cellular processes in response to calcium (*10*−*12*). The list of known CaM-dependent proteins is extensive, exceeds 300 in number (*13*−*15*), with the diversity of targets being strictly dependent on the ability of CaM to interact with its targets in different ways (*11*, *15*−*17*).

The best known mode of interaction of CaM with the target is the classical wrap-around mode with the target peptide engulfed in a hydrophobic channel (*18*) and the two lobes of CaM coming close to one other (*18*−*21*). Although the wrap-around binding model was initially assumed to be the predominant structural mechanism for CaM binding to its targets, a growing body of evidence demonstrated that CaM can also bind to targets in an unusual compact or extended conformations in some instances with less than a full complement of bound calcium ions, as well as with novel stoichiometries (*10*, *20*). In the case of the plasma membrane Ca^{2+}-pump, $4Ca^{2+}$-CaM binding to its peptide C20W involves only the C-terminal lobe, as a consequence of a missing hydrophobic anchor residue with respect to the common target sequences (*22*). A radically novel target-binding mode has been revealed with the crystal structure of $2Ca^{2+}$-CaM in complex with a fragment of K^+-channel (*23*) and exotoxin from *Bacillus anthracis* (*23*). In all these structures, CaM maintains an extended, open conformation after binding to its target.

Our *in vitro* fluorimetric analyses clarified that both the bovine inhibitor protein of F_OF_1ATP synthase IF_1 and yeast inhibitors IF_1 and STF_1 interact with Ca^{2+}-saturated CaM with a 1:1 ratio

[†]This work was supported by Italian MIUR grants, PRIN 2007, and FIRB Italian Human ProteomeNet Project 2007. MRC Medical Research Council (Centre Cambridge) is acknowledged for having kindly provided bovine IF1 protein in accordance with the Material Transfer Agreements made among MRC, University of Udine, and University of Napoli "Federico II".

*To whom correspondence should be addressed: Department of Organic Chemistry and Biochemistry, University of Napoli "Federico II", via Cynthia 6, 80126 Napoli, Italy. Tel: +39-081-674114. Fax: +39-081-674113. E-mail: birolo@unina.it.

[1]Abbreviations: CaM, calmodulin; CNBr, cyanogen bromide; EDAC, 1-ethyl-3-(3-dimethylamino-propyl)-carbodiimide; TFA, trifluoroacetic acid.

 Published on Web 07/29/2010

over a wide pH range. Moreover, sequence visual inspection, together with binding studies of CaM with bovine IF_1 synthetic peptides, revealed the presence of a conserved putative CaM-binding motif within the N-terminal of IF_1 from bovine and yeast (*2*).

In addition, we have reported that IF_1 expressed on the cell surface colocalizes with CaM in human HepG2 cells (*25*), suggesting the hypothesis that the interaction may occur *in vivo* at this level. Such a hypothesis is reinforced by recent reports documenting that IF_1 located on the plasma membrane is able to regulate the activity of F_OF_1ATP synthase expressed on the cell surface (*25*−*27*).

As mentioned above, IF_1 exists in two oligomeric states depending on pH: an inactive, highly helical, tetrameric form above pH 6.7 and an active, inhibitory, dimeric form below pH 6.7 (*3*). In the IF_1 dimer, the two monomers associate through an extended antiparallel α-helical coiled-coil in the C-terminal region, while the inhibitory active portion is in the N-terminal region (*28*). Structural data are needed in order to understand whether the binding of CaM overlaps the inhibitory portion as well as the stoichiometry of the IF_1−CaM complex. The aim of the present work was to characterize the complex between IF_1 and Ca^{2+}-CaM, by defining the stoichiometry and topology of the protein complex, in the experimental conditions in which the IF_1 is in the dimeric, inhibitory form, i.e., pH 5.

We investigated the stoichiometry of the IF_1−CaM complex by native ESI-MS analyses. Complex topology was investigated by a combined strategy, which integrates limited proteolysis and cross-linking experiments with mass spectrometric analyses.

Our data indicated that IF_1 and CaM in the physiological micromolar range form a 1:1 complex, with four calcium ions bound, and clearly demonstrated that only the C-terminal lobe of CaM is involved in the formation of the complex and contacts IF_1 within the inhibitory, flexible N-terminal region.

MATERIALS AND METHODS

Materials. Recombinant IF_1 was provided by MRC Medical Research Council (Centre Cambridge). Recombinant bovine calmodulin, TPCK treated trypsin, endoprotease Glu-C, chymotrypsin, the cross-linking reagent 1-ethyl-3-(3-dimethylaminopropyl)-carbodiimide (EDAC), α-cyano-4-hydroxycinnamic acid, and sinapinic acid were purchased from Sigma. Acetonitrile was HPLC-grade from Baker.

Biotinylation of IF_1. IF_1 (344 μg, in 50 mM MES, pH 5.0) was incubated with 8 μg of Sulfo-NHS-Biotin (sulfosuccinimidobiotin) (Pierce) (molar ratio 1:1), dissolved in the same buffer, on ice in the dark for 2 h. The reaction was stopped with 0.1 M Tris at pH 7.0, and the excess of nonreacted biotin reagent was removed by size exclusion chromatography on PD-10 columns (GE-Healthcare) in 0.1 M sodium phosphate at pH 7.2 and 0.15 M NaCl, following absorbance at 220 and 280 nm to single out IF_1-containing fractions. These fractions were pooled, and the extent of biotinylation was verified by ESI-MS on an aliquot corresponding to ~1 nmol of IF_1 protein previously purified by reverse-phase HPLC on a ZORBAX Eclipse XDB-C8 column (150 × 4.6 mm, 80 Å pore size) with a 25−65% acetonitrile linear gradient in 0.1% TFA over 10 min, at a flow rate of 1 mL/min. Elution was monitored at 220 nm, and individual fractions were collected and analyzed by electrospray mass spectrometry on a QUATTRO Micro LC-MS/MS system equipped with a Z-SPRAY source and a triple quadrupole analyzer (Waters-Micromass). Protein solution was injected into the ion source at a flow rate of 10 μL/min. Calibration of the instrument was achieved with the multicharge distribution of the equine myoglobin. Data were elaborated using the MassLynx program (Waters-Micromass).

Immobilization of Biotinylated PHK on Avidin and the Pull Down Assay. Two hundred microliters of avidin agarose resin (settled gel, Pierce) was equilibrated with five volumes of binding buffer (0.1 M sodium phosphate at pH 7.2 and 0.15 M NaCl) and incubated with biotinylated IF_1 (2 mg of biotinylated IF_1 per mL of settled avidin agarose resin) at 4 °C for 1 h. The resin was washed with 10 volumes of 50 mM MES at pH 5.0.

CaM (200 μL, 5 μM in 50 mM MES, pH 5.0) was incubated with 200 μL of biotinylated-IF_1 immobilized on avidin agarose resin and incubated overnight at 4 °C. The resin was washed with 10 volumes of 50 mM MES at pH 5.0, and the retained species were eluted with 30 μL of denaturing buffer (15.6mM Tris, 1.25% SDS, 2.5% Glycerol, 0.2M DTT). Samples were analyzed by SDS−PAGE (12.5%−10 cm × 10 cm), and proteins were stained with Coomassie Brilliant Blue G-Colloidal (Pierce, Rockford, USA).

Gel Filtration. Gel filtration experiments were carried out as follows: 50 μL of the 20 μM sample in 50 mM ammonium acetate at pH 5.0, 0.15 M NaCl, and 100 μM $CaCl_2$ were loaded on a Superdex 75 PC (3.2 × 300 mm) gel filtration column installed on Smart System (Pharmacia LKB) and isocratically eluted at 25 °C at a flow rate of 75 μL/min. The column had been previously calibrated in 50 mM sodium phosphate at pH 7.5 and 0.15 M NaCl with the following proteins of known molecular mass: bovine serum albumin (66000 Da), ovalbumin (45000 Da), carbonic anhydrase (29000 Da), trypsinogen (24000 Da), and cytochrome *c* (12400 Da).

Native Mass Spectrometry. IF_1 and the IF_1−calmodulin mixture (1/1, mol/mol) were analyzed on a Q-TOF hybrid mass spectrometer equipped with a nano Z-spray source (Waters, Manchester, UK). Protein solutions, 10 μM in 10 mM ammonium acetate at pH 5.0 and 100 μM $CaCl_2$, were injected into the ion source at a flow rate of 1 μL/min. Data were elaborated using the MassLynx program (Waters-Micromass). Calibration of the instrument was achieved with the multicharge distribution of the bovine pancreatic tripsinogen.

Complementary Proteolysis Experiments. Enzymatic hydrolyses were performed at 37 °C by incubating the 10 μM sample in 10 mM ammonium acetate at pH 5.0 and 100 μM $CaCl_2$ with either trypsin, chymotrypsin, or endoprotease Glu-C, enzyme-to-substrate ratios ranging from 1:4000 to 1:100 (w/w). The extent of proteolysis was monitored on a time-course basis by sampling the reaction mixture at different time intervals from 1 to 60 min and directly analyzing the released peptides by MALDI-MS. For each measurement, an aliquot of 1 μL of peptide mixture was applied to a sample slide and mixed with 4 μL of a 10 mg/mL sinapinic acid solution in acetonitrile/0.2% TFA (70:30, v/v) before air drying. The samples were then analyzed on a linear Voyager DE MALDI-TOF mass spectrometer (Applied Biosystems, Foster City, CA). The mass range was internally calibrated with the $[M + H]^+$ and $[M + 2H]^{2+}$ ions from the entire IF_1 protein present in the proteolytic mixture.

Chemical Cross-Linking Experiments. Cross-linking reactions on the IF_1 dimer were carried out in a total volume of 20 μL of 50 mM MES at pH 5.0. IF_1 (0.5 nmol) was incubated at 37 °C for 15 min and then treated with 1-ethyl-3-(3-dimethylamino propyl)-carbodiimide (EDAC) cross-linking reagent for 30 min.

Cross-linking reactions on the IF_1−calmodulin complex were carried out in a total volume of 20 μL of 50 mM MES at pH5.0,

1 mM $CaCl_2$, and 0.15 M NaCl. Then, 0.5 nmol of IF_1 and 0.5 nmol of CaM were incubated at 37 °C for 15 min and then treated with 1-ethyl-3-(3-dimethylamino propyl)-carbodiimide (EDAC) cross-linking reagent for 30 min.

Preliminary experiments were carried out both for the IF_1 dimer and the IF_1−CaM complex to determine the optimal excess of EDAC. Cross-linking reactions were terminated by quenching the excess of reagents with gel loading buffer (15.6 mM Tris-HCl, 1.25% SDS, 2.5% glycerol at pH 6.8, and 0.2 M DTT). The protein samples were heated at 100 °C for 5 min and separated by electrophoresis on a 15% SDS−polyacrylamide gel. Proteins were detected by colloidal Coomassie, and selected positively stained protein bands were excised from the gel, *in situ* digested with trypsin, and analyzed by MALDI-MS for protein identification.

In IF_1 dimer cross-linking experiments on a preparative scale, 6 nmol in 120 μL of IF_1 were incubated at 37 °C for 15 min and then treated with a 10-fold molar excess of EDAC for 30 min at 37 °C. The reaction was stopped by acidification with 1% TFA. The cross-linked protein was purified by reverse-phase HPLC on a ZORBAX Eclipse XDB-C8 column (150 × 4.6 mm, 80 Å pore size) with a 15−65% acetonitrile linear gradient in 0.1% TFA over 30 min, at a flow rate of 1 mL/min. Elution was monitored at 220 nm, and individual fractions were collected and analyzed by electrospray mass spectrometry on a QUATTRO Micro LC-MS/MS system equipped with a Z-SPRAY source and a triple quadrupole analyzer (Waters-Micromass). Protein solution was injected into the ion source at a flow rate of 10 μL/min. Data were elaborated using the MassLynx program (Waters-Micromass). The cross-linked protein fraction was evaporated to dryness in a Speed Vac concentrator (Savant), resuspended in 10 mM ammonium bicarbonate at pH 8.0, digested with trypsin at 37 °C (E/S, 1:50 (w/w)) overnight, and subjected to MALDI-MS and LC-MS/MS analysis.

In the cross-linking experiment, the IF_1−CaM complex on a preparative scale, 15 nmol of both IF_1 and calmodulin was incubated in 400 μL of 50 mM MES at pH 5, 1 mM $CaCl_2$, and 0,15 M NaCl at 37 °C for 15 min and then treated with a 10-fold molar excess of EDAC for 30 min. The reaction was stopped by acidification with 1% TFA. The cross-linked protein was purified by reverse-phase HPLC on a Phenomenex Jupiter C4 column (250 × 4.6 mm, 300 Å pore size) with a linear gradient of 5−65% acetonitrile in 0.1% TFA over 40 min, at a flow rate of 1 mL/min. Elution was monitored at 220 nm, and individual fractions were collected and analyzed by electrospray mass spectrometry on a Quattro-Micro triple quadrupole mass spectrometer (Waters-Micromass). Protein solution was injected into the ion source at a flow rate of 10 μL/min. Data were elaborated using the MassLynx program (Waters-Micromass). The cross-linked protein fraction was digested with CNBr in 70% TFA overnight at room temperature under an inert atmosphere in the dark using a large weight excess of the reagent over protein. The sample was then diluted 10-fold with water and evaporated to dryness in a Speed Vac concentrator (Savant). The sample was then fractionated by reverse-phase HPLC on a Phenomenex Jupiter C4 column (250 × 2.00 mm, 300 Å pore size), and individual fractions were collected and analyzed by electrospray mass spectrometry. Selected fractions were digested with trypsin in 50 mM ammonium bicarbonate at pH 8 at 37 °C (E/S, 1:50 (w/w)) overnight and subjected to MALDI-MS and LC-MS/MS analysis.

MALDI mass spectra were recorded on an Applied Biosystems Voyager DE-PRO mass spectrometer equipped with a reflectron analyzer and used in delayed extraction mode. One microliter of the peptide sample was mixed with an equal volume of α-cyano-4-hydroxycynnamic acid as matrix (in acetonitrile/50 mM citric acid (70:30, v/v)), applied to the metallic sample plate, and air-dried. Mass calibration was performed by using the standard mixture provided by the manufacturer.

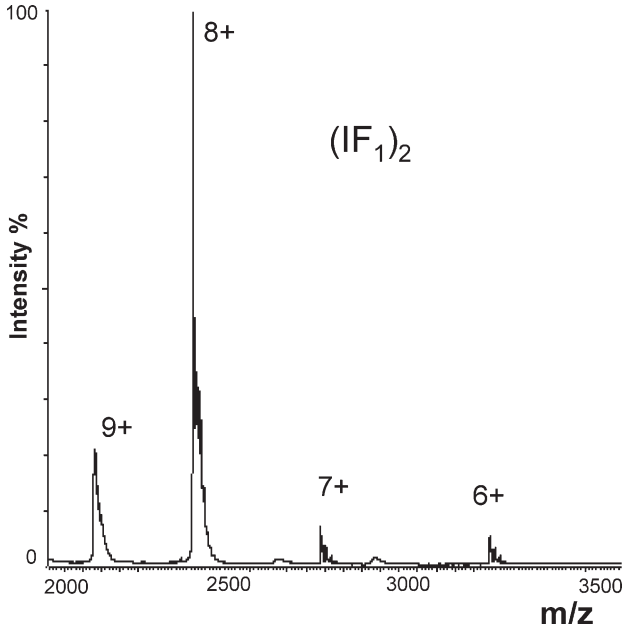

FIGURE 1: Native ESI-MS mass spectrum of the IF_1 dimer, showing the predominant dimeric ions.

LC-MS/MS analyses were performed on a Q-TOF hybrid mass spectrometer equipped with a Z-spray source and coupled online with a capillary chromatography system CapLC (Waters, Manchester, UK). After loading, the peptide mixture (4 μL) was first concentrated and washed at 10 μL/min onto a reverse-phase precolumn using 0.2% formic acid as eluent. The sample was then fractionated onto a C18 reverse-phase capillary column (75 μm × 20 mm) with 10−50% acetonitrile in 0.2% formic acid over 40 min, at a flow rate of 280 nL/min. The mass spectrometer was setup in a data-dependent MS/MS mode where a full scan spectrum (m/z acquisition range from 400 to 1400 Da/e) was followed by a tandem mass spectrum (m/z acquisition range from 100 to 2000 Da/e). Peptide ions were selected as the three most intense peaks of the previous scan. Suitable collision energy was applied depending on the mass and charge of the precursor ion.

RESULTS

Structural Characterization of IF_1. Oligomeric State of IF_1. The oligomeric state of IF_1 was assessed by direct ESI-MS measurement under native conditions. An aliquot of IF_1 (20 μM) was incubated in 10 mM ammonium acetate at pH 5.0 at 37° for 30 min and then directly injected into the electrospray source of a hybrid Q-TOF type mass spectrometer. Figure 1 shows the multiply charged ion spectrum of native IF_1, showing the presence of mass signal distribution encompassing $z = +9$ to $z = +6$ ions. The measured molecular mass calculated from the ESI-MS spectrum was 19166.3 ± 0.3 Da, in excellent agreement with the expected value for a dimeric IF_1 species ($(IF_1)_2$ = 19163 Da).

Limited Proteolysis. Limited proteolysis experiments were designed to study the surface topology of $(IF_1)_2$ on the grounds that the portions of the protein that are involved in highly

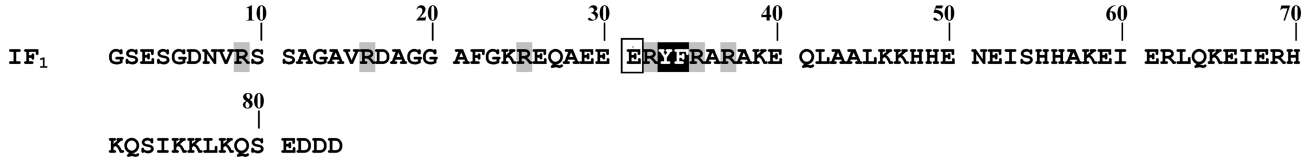

FIGURE 2: Preferential cleavage sites observed in the dimeric form of IF_1. The diagram shows the results obtained with trypsin (highlighting in gray), chymotrypsin (highlighting in black), and Glu-C (boxed residue). In all cases, the proteolytic cleavage took place between the indicated residue and the following one in the sequence.

Table 1: Peptides Generated in the Digestions of the Dimeric Form of IF_1 with Proteases and Identified by MALDI-TOF Analysis

protease (enzyme/IF1 ratio, w/w)	identified peptide	experimental $[MH^+]$ mass value (Da)	theoretical $[MH^+]$ mass value (Da)
Glu-C (1/400)	1−31	3125.69	3125.19
	32−84	6476.55	6476.28
trypsin (1/500)	1−9	919.70	920.90
	1−16	1548.81	1549.59
	1−25	2409.17	2409.52
	1−32	3281.35	3281.38
	1−35	3748.26	3747.92
	1−37	3975.7	3975.19
	38−84	5626.54	5626.29
	36−84	5853.75	5853.56
	33−84	6319.74	6320.10
	26−84	7191.11	7191.95
	17−84	8051.82	8051.89
	10−84	8680.66	8680.58
chymotrypsin (1/1000)	1−33	3444.10	3444.56
	1−34	3591.45	3591.73
	35−84	6009.01	6009.75
	34−84	6156.44	6156.92

structured regions or are located at the intersubunits interface are protected from proteases (*29*).

$(IF_1)_2$ (20 μM) was individually incubated with trypsin, chymotrypsin, or endoprotease Glu-C, as conformational probes. The extent of the enzymatic hydrolysis was monitored on a time-course basis by sampling 1 μL aliquots of the incubation mixture at different interval times followed by MALDI-MS analysis. Fragments released from the dimer were identified on the basis of their unique mass values and the specificity of the proteolytic enzyme. Identification of the two complementary peptides following a single proteolytic event led to the assignment of the preferential cleavage sites (*29*). In Supporting Information, an example of the MALDI-TOF analysis of the time course experiments with Glu-C endoprotease is reported.

The overall results of the limited proteolysis experiments are summarized in Table 1 and Figure 2, from which a number of considerations can be drawn. Preferential cleavage sites in $(IF_1)_2$ gathered into specific regions of the protein, the most exposed segment being the N-terminal portion spanning Glu31−Arg37. Interestingly, no cleavage sites were detected in the C-terminal region. These data are in perfect agreement with NMR data on the 44−84 C-terminal coiled-coil IF_1 domain (*30*), and with the crystallographic structure of the IF_1 mutant H49K (*1*) that could not be resolved in the N-terminal portion due to the high flexibility of this region. The high resolution data depict a central, highly structured, and, therefore, likely inaccessible, antiparallel coiled-coil structure formed by the opposite pairing of the two C-terminal regions with the two, very flexible and exposed N-terminal arms protruding at each end. This structural organization perfectly justifies our results.

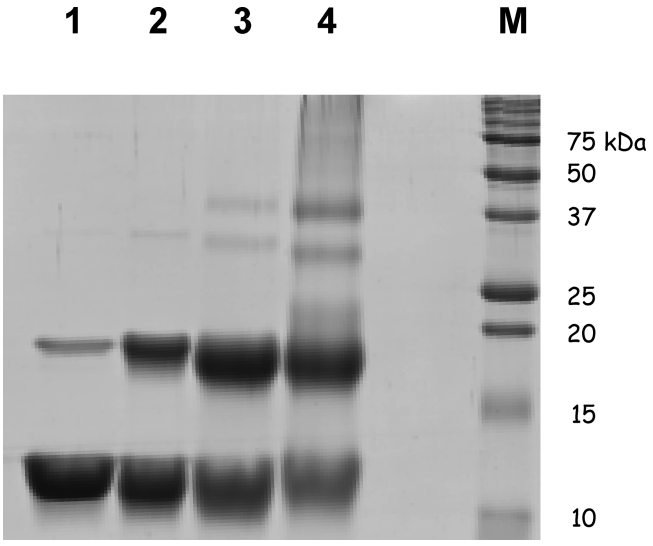

FIGURE 3: $(IF_1)_2$ cross-linking with EDAC. SDS−PAGE of reaction mixtures with different $(IF_1)_2$/EDAC ratios: (1) $(IF_1)_2$ without EDAC; (2) $(IF_1)_2$/EDAC 1/10; (3) $(IF_1)_2$/EDAC 1/100; (4) $(IF_1)_2$/EDAC 1/500; (M) protein molecular weight markers; molecular weights are reported in kDa on the side. All of the reactions were carried out at 37 °C for 30 min in 50 mM Na-MES at pH 5.0 and stopped by the addition of the SDS−PAGE sample buffer.

Chemical Cross-Linking of $(IF_1)_2$. The interacting contact regions in the IF_1 dimer complex were further investigated by chemical cross-linking. Cross-links were introduced with the heterobifunctional reagent EDAC (1-ethyl-3-(3-dimethylaminopropyl) carbodiimide) that forms zero-length isopeptidic bonds between the carboxylic group of Glu residues and the ε-amino group of lysines or the free N-terminus of the protein.

$(IF_1)_2$ (20 μM) was incubated in 50 mM MES buffer at pH 5.0 and treated with EDAC at 37 °C. Several concentrations of EDAC and different reaction times were tested and the final experimental conditions were accurately selected to result solely in the formation of dimeric species, avoiding the formation of high molecular mass oligomers and distortion of the tertiary structure by excessive cross-linking. The cross-linking reaction mixtures were separated by monodimensional SDS−PAGE and the resulting gel stained with colloidal Coomassie Blue. Figure 3 shows the electrophoretic analysis of $(IF_1)_2$ treated with 10, 100, 500 molar excess of EDAC for 30 min at 37 °C. A protein band with an apparent molecular mass of 19 kDa was clearly detected in lanes 2, 3 and 4, which could tentatively be assigned to a covalent dimer of IF_1. IF_1 was also analyzed on the gel without treatment with EDAC as the control (Figure 3, lane 1). A thin band corresponding to a dimeric species could also be observed in these conditions, demonstrating the peculiar stability of the noncovalent $(IF_1)_2$ dimer, which can resist even to the highly denaturant conditions of the SDS−PAGE analysis. A 10-fold molar excess of EDAC was considered enough to introduce cross-links in a sufficient amount to freeze the dimeric IF_1 species

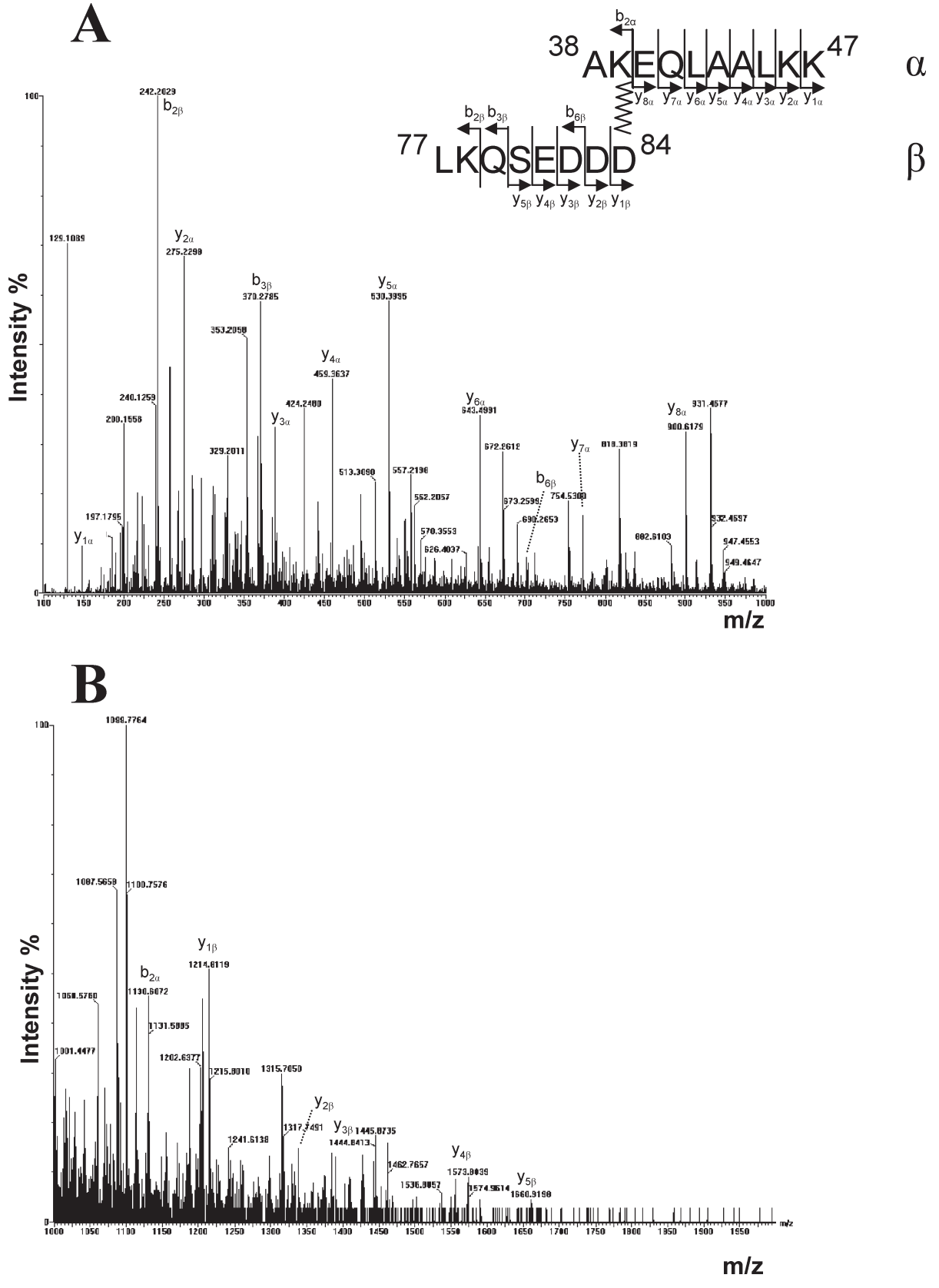

FIGURE 4: MS/MS spectra of the cross-linked peptides AKEQLAALKK and LKQSEDDD. Tandem mass spectra of the precursor ion $[M + 3H]^{3+} = 677.4$. Fragments from the peptide AKEQLAALKK are labeled with an α subscript and those from peptide LKQSEDDD with a *β* subscript. Most ion assignments are indicated on the peptide sequence in the figure. Panels A and B represent enlargements of different mass ranges of the same MS/MS spectrum.

for subsequent analysis, while higher excesses of EDAC generated higher molecular weight bands, thus suggesting aggregation of the protein caused by excessive cross-linking.

The dimeric protein band was excised from lane 2 and subjected to enzymatic in-gel digestion with trypsin. For comparative purposes, the monomeric IF_1 band from the reference sample

(lane 1) was also excised and treated in the same manner. The tryptic digests were then analyzed by MALDI-MS, and the experimentally obtained mass values were mapped onto the anticipated IF_1 sequence, confirming the identity of the protein bands and the absence of any contaminants.

The MALDI-MS fingerprint of dimeric IF_1 showed the occurrence of three signals that could be assigned to putative cross-linked products. The signal at m/z 2030.1 was assigned to the cross-linked peptides 38−47 and 77−84; the signal at m/z 2257.2 was interpreted as arising from either the peptide 36−47 linked to the peptide 77−84 or the peptide 36−46 joined to the peptide 76−84; the signal at m/z 3349.7 was assigned to the peptides 38−58 and 77−84. Although the IF_1 regions involved in the cross-link were clearly outlined by these data, discrimination on which amino acids were actually covalently linked could not be obtained by MALDI-MS data. A second aliquot of cross-linked IF_1 was then purified by HPLC and analyzed by ESI-MS providing the expected molecular mass of 19145.7 ± 0.7 Da. The sample was digested with trypsin and the resulting peptide mixture analyzed by nano LC-MS/MS. The multiply charged ions corresponding to the putative cross-linked species were isolated and fragmented by collision induced dissociation (CID). An example of the quality of the data is provided in Figure 4 where the fragmentation spectra of the triply charged ion at m/z 677.4 (corresponding to the MH^+ 2030.1) are shown.

The daughter ion spectra exhibited almost the entire y ion series for the two peptides 38−47 and 77−84. The $y_{1\beta}$ and $y_{8\alpha}$ ions constituted the key signals to assess the covalently linked residues. The former corresponds to the entire 38−47 peptide linked to Asp84, whereas the latter represents the residual 40−47 fragment following the release of Asp84 and the dipeptide Ala38-Lys39.

These data unequivocally indicated that the cross-linked species consisted of peptides 38−47 and 77−84 covalently linked by an isopeptide bond joining Asp84 to Lys39. Tandem mass spectra of ions corresponding to the other signals identified in the MALDI-MS analysis of the tryptic digests confirmed Asp84 and Lys 39 as the aminoacids involved in the cross-linked product. This isopeptide bond does not fit with the data of the IF_1 crystal structure. However, fragmentation spectra reported in Figure 4 can be unequivocally interpreted as such. The apparent discrepancy could be explained taking into account the conditions of our experiments, performed in solution at pH 5 and at low IF_1 concentration, rather different from the crystallization ones. Moreover, as stated by Walker's group (*3*), the region in wild-type IF_1 predicted to be in the coiled-coil extends from residues 37 to 84, consistent with our experimental observation, whereas for the IF1-H49K mutant, for which the three-dimensional structure has been solved at high resolution (*1*), the coiled-coil region is predicted to be shorter (involving only residues 47−84), in good agreement with the structural data. It should be noted that we worked with the wild-type IF_1 only, thus possibly explaining the discrepancy between the cross-linked residues observed and the high resolution data.

Structural Characterization of the IF_1−CaM Complex. IF_1−CaM Pull Down. The existence of a IF_1−CaM complex, as suggested by the Pedersen and Carafoli groups (*4*, *5*) and characterized by spectroscopic analysis (*2*) was further preliminarily assessed by a pull down assay exposing immobilized biotin labeled IF_1 to CaM.

Biotinylation of IF_1 was carried out with Sulfo-NHS-Biotin (sulfosuccinimidobiotin) and Biotin-IF_1 was immobilized on avidin, as described in the Materials and Methods. An aliquot

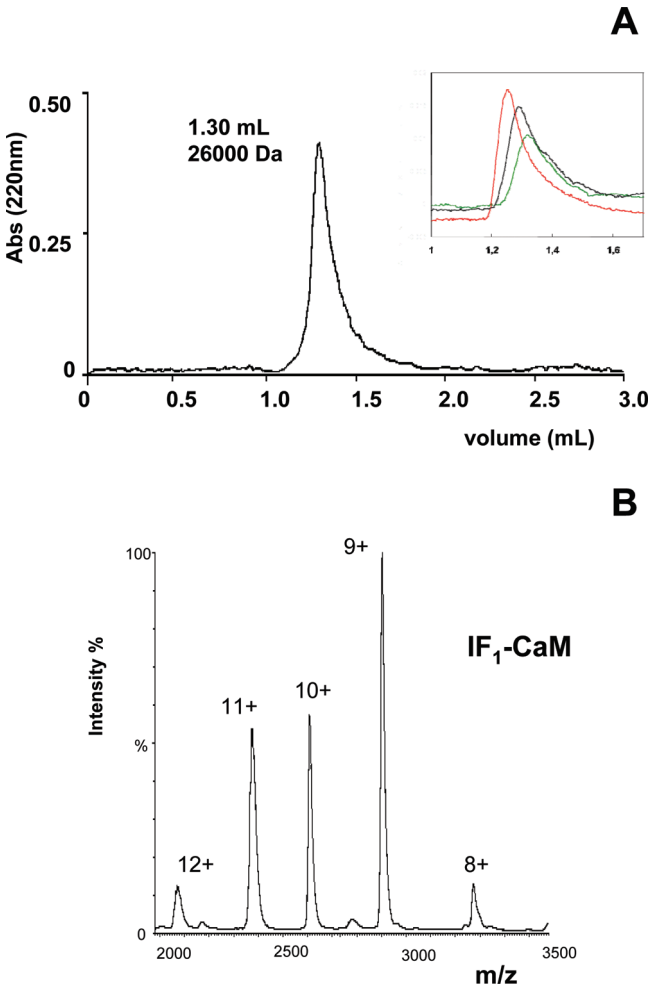

FIGURE 5: IF_1−CaM complex is a heterodimer. (A) Size exclusion chromatography on a Superdex-75 column of an equimolar mixture of IF_1 and CaM. In the inset, a zoom of the elution profile of IF_1−CaM (black line) is overlaid on those of isolated $(IF_1)_2$ (red line) and CaM (green line) obtained in the same chromatographic conditions (50 mM ammonium acetate at pH 5.0, 0.15 M NaCl, and 100 μM $CaCl_2$). (B) Native ESI-MS mass spectrum of the IF_1−CaM complex, showing the predominant heterodimeric ions.

of Biotin-IF_1 was purified by RF-HPLC an analized by ES-MS in order to assess the biotinilation yield showing that in the experimental conditions used IF_1 was efficiently biotinylated (up to 2 biotins per IF_1 monomer).

The biotinylated IF_1 was immobilized on avidin beads that were subsequently incubated with CaM in 50 mM MES buffer at pH 5.0. After extensive washing, the CaM that had been recruited by immobilized IF_1 was eluted in denaturing buffer, separated on SDS−PAGE and stained with colloidal blue Coomassie (Figure S2, Supporting Information). In a control experiment, an aliquot of CaM was loaded on avidin beads in the absence of immobilized IF_1, and treated as above: no CaM was unspecifically retained by avidin beads, thus unequivocally demonstrating the existence of a specific interaction between IF_1 and calmodulin.

Stoichiometry of the IF_1−CaM complex. The stoichiometry of the IF_1−calmodulin (CaM) complex was investigated by native electrospray mass spectrometry analyses. Preliminary size exclusion chromatography analysis was used to inspect the hydrodynamic behavior of the complex. Approximately equimolar amounts of IF_1 and CaM (20 μM of each protein) were incubated at 37° for 30 min at pH 5.0 and then loaded onto a Superdex 75 size exclusion column. The chromatography resulted

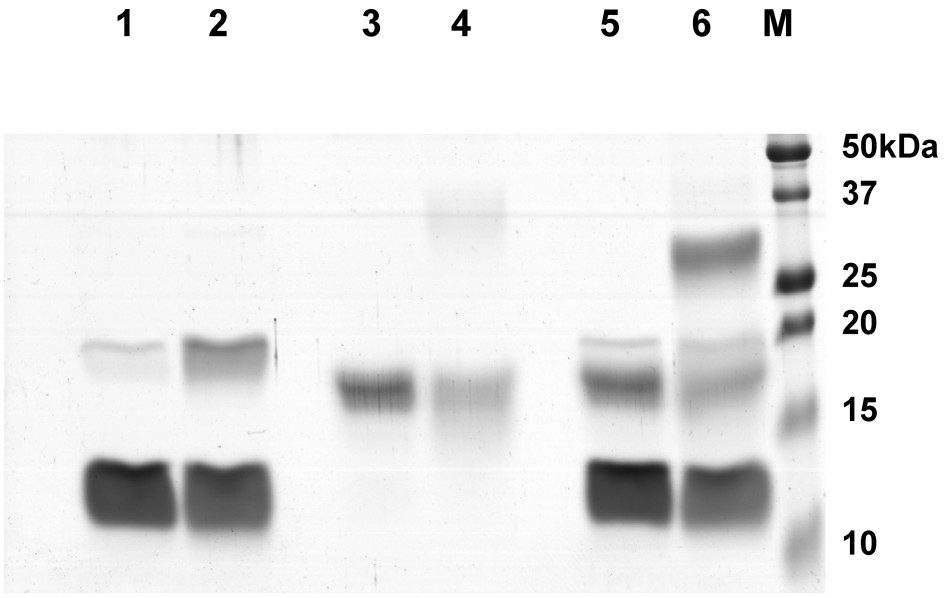

FIGURE 6: IF_1−CaM cross-linking with EDAC. SDS−PAGE of reaction mixtures of IF_1 (20 μM) and CaM (20 μM) with EDAC (200 μM). The samples are labeled as follows: (M) protein molecular weight markers, (1) CaM, (2) CaM with EDAC, (3) IF_1, (4) IF_1 with EDAC, (5) IF_1 and CaM mixture, and (6) IF_1 and CaM mixture with EDAC. All of the reactions were carried out at 37 °C for 30 min in 50 mM Na-MES at pH 5.0 and stopped by the addition of the SDS−PAGE sample buffer.

in a single peak, which eluted at an apparent molecular mass of about 26000 Da (Figure 5, panel A; elution volume, 1.30 mL; see the inset in the figure), suggesting a 1:1 stoichiometry of the complex. Peak top fractions were analyzed by MALDI-TOF, revealing the presence of both proteins, i.e., IF_1 and CaM (data not shown). Most importantly, no peak eluting at a volume corresponding to a higher apparent molecular weight was observed, thus suggesting that, in these experimental conditions, the complex is present in a single predominant homogeneous oligomeric state. However, a reliable definition of the stoichiometry of the complex from size exclusion analysis is impaired by the elongated shape of both components, which significantly alters the hydrodynamic behavior of the two isolated proteins (in the same experimental conditions, $(IF_1)_2$ elutes with an apparent molecular weight of 30000 Da (Figure 5, panel A; elution volume, 1.25 mL; see the inset in the figure) and CaM with an apparent molecular weight of 23000 Da (Figure 5, panel A; elution volume, 1.32 mL; see the inset in the figure), in fairly good agreement with the apparent molecular weight reported by other authors (*31*, *32*)).

Therefore, this issue was further addressed by native mass spectrometry, which is not affected by the elongated conformation of the singular components. An equimolar amount of the two proteins (20 μM of each protein) was mixed at 37° for 30 min and then directly injected into the electrospray source of a hybrid Q-TOF type mass spectrometer under native conditions. Panel B in Figure 5 shows the enlargement of the full spectrum exhibiting the presence of a clear distribution of mass signals encompassing $z = +12$ to $z = +8$ ions that was assigned to the IF_1−CaM complex containing 4 calcium ions. The measured molecular mass of this species was 26527.3 ± 0.7 Da, in excellent agreement with the expected value for one IF_1 molecule bound to one CaM molecule bearing four calcium ions (expected molecular mass = 26528.0 Da). This result clearly indicated a 1:1 stoichiometry for the IF_1−CaM complex.

Chemical Cross-Linking. The interacting regions in the IF_1−CaM complex were investigated by chemical cross-linking with the heterobifunctional reagent EDAC, using a procedure similar to the procedure described above for the IF_1 dimer.

IF_1 and CaM (20 μM of each protein) were incubated as reported in the Materials and Methods section, and then treated with a 10-fold molar excess of EDAC at 37 °C for a further 30 min. Isolated CaM and IF_1 were also individually incubated with EDAC under the same conditions as the control. Several concentrations of EDAC and different reaction times were tested, and the final experimental conditions were accurately selected to result in the formation of an IF_1−CaM heterodimeric complex, avoiding the formation of high molecular mass oligomers and preventing excessive cross-linking.

The different mixtures of products generated by the cross-linking reaction were analyzed by SDS−PAGE, as shown in Figure 6 for the reaction carried out with a 10-fold molar excess of EDAC. A protein band with an apparent molecular mass of 26 kDa was clearly detected in lane 6. This band was absent both when equimolar amounts of IF_1 and CaM were mixed without the cross-linking reagent (lane 5) and when CaM and IF_1 were individually treated with EDAC (lanes 2 and 4, respectively). Aggregation of proteins caused by excessive cross-linking was not observed as demonstrated by the absence of any band in the higher mass range.

The identity of the 26 kDa gel band was definitively assessed by identification of the protein components by mass spectral analysis. The protein band was excised from the gel and subjected to enzymatic in-gel digestion with trypsin. The resulting peptide mixture was directly analyzed by MALDI-MS and the corresponding mass values were mapped onto the anticipated sequences of IF_1 and CaM revealing the contemporaneous presence of both proteins. These results strongly supported the formation of a covalent IF_1−CaM complex following EDAC treatment and confirmed previous mass spectral data on the stoichiometry of the complex.

A second aliquot of the cross-linked IF_1−CaM complex was fractionated by reverse phase HPLC and the collected fractions analyzed by ESI-MS. The covalent IF_1−CaM complex eluted in two fractions exhibiting molecular masses of 26353.5 ± 1.0 Da and 26336.1 ± 1.6 Da, the latter being a minor component. These mass values correspond to the molecular masses of the two

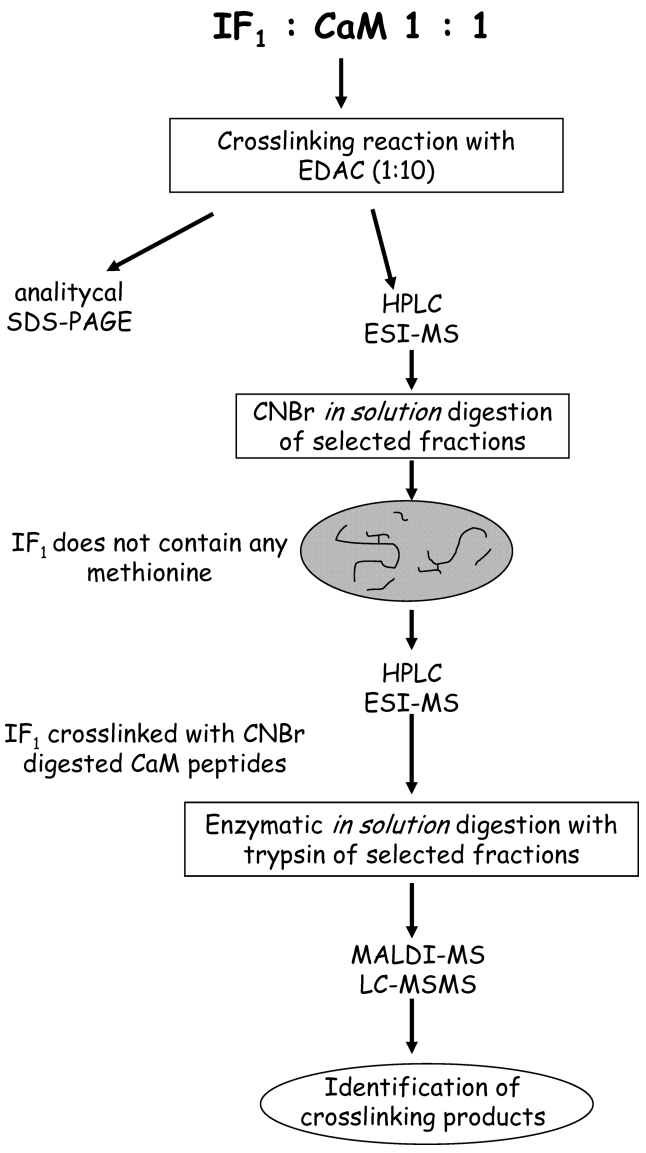

FIGURE 7: General analytical strategy for mapping the interaction between IF_1 and CaM by chemical cross-linking.

proteins minus 18.01 and 36.02 Da, indicating the presence of the 1:1 IF_1−CaM complex containing one and two cross-linking bonds.

Identification of the cross-linked residues in both IF_1 and CaM proteins was achieved following the strategy outlined in Figure 7 on the fraction containing the IF_1−CaM species where one covalent cross-link had been introduced. The rationale behind this strategy is based on the absence of methionine residues in the IF_1 sequence that is then unreactive with CNBr. Chemical hydrolysis of the complex would have therefore left the undigested IF_1 molecule covalently linked to CaM peptides, making these fragments immediately detectable by mass spectrometry.

The complex was then subjected to CNBr hydrolysis in 70% TFA at room temperature overnight, and the resulting peptide mixture was fractionated by HPLC. Individual fractions were manually collected and directly analyzed by ESI-MS. The fraction containing the species with a molecular mass 11280.2 ± 0.5 Da could be tentatively interpreted as IF_1 linked to peptide 110−124 of CaM (theoretical mass value 11280.3 Da). Two minor fractions containing the species with a molecular mass of 13560.3 ± 0.6 Da and 15063.0 ± 0.9 Da were also observed and interpreted as IF_1 linked to peptides 110−144 and 77−124, respectively (corresponding theoretical mass values of 13560.8 and 15061.5 Da, respectively).

The major component was further hydrolyzed with trypsin at 37 °C overnight, and the resulting peptide mixture directly analyzed by both MALDI-MS and nano LC-MS/MS. MALDI-MS spectra displayed the presence of three signals, at m/z 2594.1, 2636.1, and 3465.4 that could not be assigned to any linear peptide within the aminoacid sequence of either IF_1 or CaM. These species were then considered as putative cross-linked fragments and tentatively interpreted as the IF_1 peptides 17−25, 1−9, and 17−32 linked to the CaM fragment 110−124 (theoretical mass values 2594.2 Da, 2636.1 Da, and 3465.57 Da, respectively).

Validation of these hypotheses and identification of the IF_1 and CaM amino acids covalently linked were achieved by tandem mass spectrometry experiments. The peptide mixture was analyzed by nano LC MS/MS, and the multiply charged ions corresponding to the three putative cross-linked species were isolated and fragmented by collision induced dissociation (CID). Figure 8 shows the fragmentation spectra of the triply charged ion at m/z 879.3 (corresponding to the MH^+ 2636.1). The complete y-ion series attributed to the IF_1 peptide 1−9 and part of the b-ion series spanning the sequence 116−122 of the CaM fragment 110−124 could be detected, thus confirming the interpretation of the MALDI data. The specific fragmentation of the two peptides was certainly dictated by the presence of a trimethyl-lysine residue at position 115 of the CaM peptide and an Arg residue located at the C-terminus of the IF_1 fragment, both endowed with a high charge retention propensity.

The individual residues of the two proteins effectively involved in the covalent linkage could also be assessed by the MS/MS data. The two key signals in the spectrum were identified at m/z 1486.5 and 1265.5. The former belongs to the b-ion series and corresponds to the loss of the CaM Glu123-Met124 dipeptide together with the entire IF_1 1−9 fragment from the cross-linked species. On the contrary, the y-ion at 1265.5 accounts for the whole IF_1 fragment covalently bound to the CaM tripeptide Asp122-Glu123-Met124, with the positive charge retained on the Arg9 residue.

These data unequivocally indicated that the cross-linked species consisted of the 1−9 N-terminal peptide of IF_1 and the 110−124 fragment covalently linked by an isopeptide bond joining Glu123 in the CaM molecule to the IF_1 N-terminal amino group.

Similar analyses were carried out on the other two cross-linked species, demonstrating their identity as the IF_1 peptides 17−25 and 17−32 linked, respectively, to the CaM 110−124 fragment. Moreover, the cross-linked bond could be shown to involve the CaM Glu123 residue and the ε-amino group of IF_1 Lys 24.

Altogether, the cross-linking experiments pointed to an IF_1−CaM complex in which the N-terminal portion of IF_1 is in close contact with the calmodulin C-terminal lobe.

DISCUSSION

The IF_1−CaM complex was investigated in solution by a combined strategy which integrates mass spectrometric methodologies and cross-linking experiments. Crucial issues of the structural characterization were the stoichiometry of the IF_1−CaM complex and the understanding of the contact region between IF_1 and calmodulin.

Mass spectral analysis of the IF_1−CaM complex under native conditions highlighted the 1:1 stoichiometry, indicating that a single IF_1 moiety binds a single CaM molecule. Most interestingly,

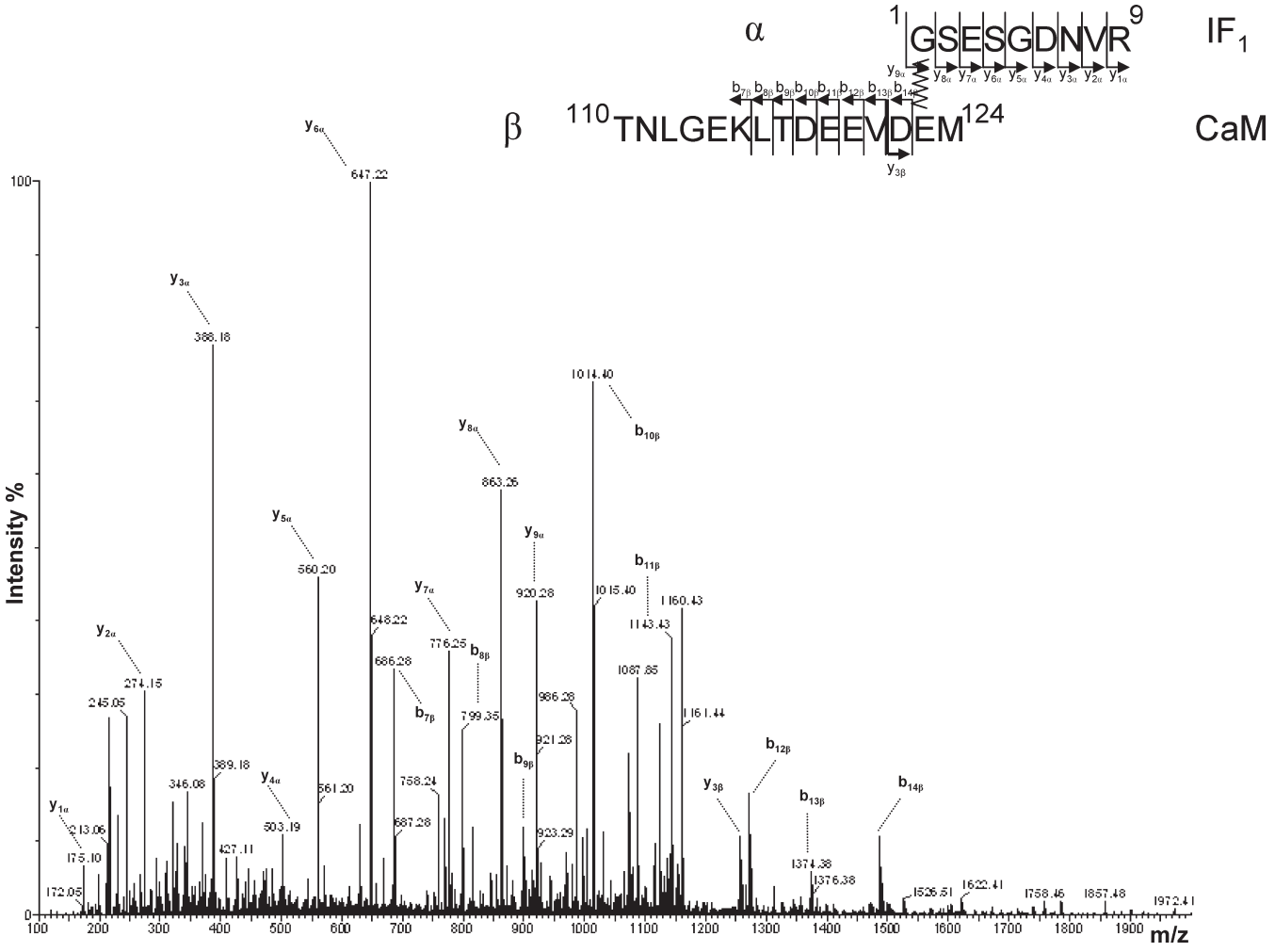

FIGURE 8: MS/MS spectra of the cross-linked peptides GSESGDNVR of IF_1 and TNLGEKLTDEEMDEM of CaM. Tandem mass spectra of the precursor ion $[M + 3H]^{3+} = 879.31$. Fragments from the peptide GSESGDNVR are labeled with an α subscript and those from peptide TNLGEKLTDEEMDEM with a β subscript. Most ion assignments are indicated on the peptide sequence in the figure.

the accurate mass value revealed that 4 Ca^{2+} ions remain bound to CaM, in accordance with the maintenance of a high Ca^{2+} affinity in the complex (*4*). The ESI-MS did not reveal the presence of higher order oligomers, as preliminarily suggested by gel filtration chromatography. The 1:1 stoichiometry implies, therefore, that CaM binds to monomeric IF_1, although IF_1 alone in solution at acidic pH exists and is functional as a dimer, as already suggested by several experimental data (*3*) and confirmed by mass spectral analysis under native conditions in the present study.

The present results, together with our previous data documenting the maintenance of a 1:1 molar ratio upon CaM fluorimetric titration with IF_1 up to 10 molar excess (*2*), are consistent with a 1:1 IF_1−CaM complex stoichiometry in the micromolar concentration range, which correlates with the physiological concentration of CaM present in living cells (8.8 ± 2.2 μM) (*33*).

More details on the IF_1−CaM interaction were needed to ascertain whether CaM might interfere with the intersubunit contacts of the IF_1 dimer or bind the inhibitory active N-terminal region of the molecule. Cross-linking experiments identified residues at the contact interface of the IF_1−CaM complex. Glu123 in the CaM molecule was shown to cross-link either the N-terminal amino group of IF_1 or the ε-amino group of IF_1 Lys24.

A merely qualitative examination of the cross-linking data suggested that a unique binding mode of IF_1 in the IF_1−CaM complex is incompatible with the experimental results since the same CaM residue (Glu123) was found cross-linked to two different IF_1 residues, suggesting the existence of at least two types of IF_1−CaM complexes, although the possibility of the spatial proximity of the IF_1 N-terminus and Lys 24 that can be alternatively cross-linked to Glu123 cannot be ruled out. In order to correctly interpret this result, it is also worth considering the ability of CaM to recognize its targets in multiple modes, as highlighted by similar experiments carried out on the well known CaM−melittin complex (*17*) where multiple modes of binding exist. Moreover, and mostly relevant in this case, the well documented (*1*) flexibility of the N-terminal region of IF_1 is an additional element that has to be taken into account to explain the multiple binding modes observed in the IF_1−CaM complex. This N-terminal segment, extending from the central coiled-coil of the molecule, appears to be essentially unstructured, as demonstrated by the high accessibility to proteases exhibited by the IF_1 dimer up to Arg 37, with the most exposed segment being the N-terminal portion spanning Glu31−Arg37. However, despite the multiple binding mode observed, it is clear that it is the N-terminal inhibitory region of IF_1 that is involved in binding to CaM, in agreement with the hypotheses that arose on the basis of sequence analysis and with the previous data obtained with synthetic peptides (*2*). The IF_1 sequence 33−42 was previously assessed as a putative target region for CaM on the basis of fluorimetric binding studies using dansyl-CaM and native bovine

IF_1 by comparing two synthetic peptides and two natural mutants, namely, yeast inhibitor proteins IF_1 and STF1 (*2*). We can consider the contact interface at the 33−42 region to be congruent with one of the multiple types of binding characterized by the cross-linking of CaM Glu123 to IF_1 Lys24.

Together, the findings that it is the N-terminal inhibitory region of IF_1 that is involved in the contact interface with CaM and that the complex stoichiometry is 1:1 suggest that binding to CaM promotes the dissociation of the active IF_1 dimer without directly interfering with the intersubunit contacts of the IF_1 dimer.

The overall cross-linking data produced in this article clearly indicate that only the C-terminal lobe of CaM is involved in binding IF_1. This definitively suggests that the IF_1−CaM complex deviates from the canonical or at least more frequent representation of CaM complexes in which the protein adopts a horseshoe-like structure with the N and C-terminal lobes, far apart in the dumbbell native protein (*34*), coming in close contact when the target peptide is bound, and originating an overall globular shaped complex.

Novel structures of CaM complexed with large target fragments, namely, the calcium-activated K^+ channel (*23*), and anthrax adenylate cyclase exotoxin (*24*) have been solved revealing unexpected binding modes, and our data clearly put the IF_1−CaM complex among the noncanonical CaM interaction mode. Moreover, a noncanonical binding mode might also explain the unchanged CaM affinity for Ca^{2+} previously observed in the complex (*2*). In the more common binding mode, the dissociation constants of Ca^{2+} from the EF hands of CaM in both C-terminal and the N-terminal lobes decrease significantly as a consequence of ternary complex formation (*35*−*37*).

Therefore, the IF_1−CaM complex can be included in the category of novel structures of CaM−target complexes. Interestingly, Vetter and Leclerc reported that in the case of a Ca^{2+} pump, the complex only involved the C-terminal lobe of CaM, similar to what occurs in the IF_1−CaM complex (*20*). In particular, NMR analysis of CaM complexed with the C20W peptide of the Ca^{2+} pump, showed that the protein remained in an extended conformation with a flexible central linker region between Arg74 and Glu84, thus explaining the changes in fluorescence emission spectra of Lys75-dansylated CaM upon binding to the C20W peptide (*20*). Similarly, the binding of Lys75-dansylated CaM to IF_1 showed changes in the fluorescence emission suggesting that the linker region of CaM responded with conformational changes to IF_1 binding (*2*).

The involvement of only the C-terminal lobe of CaM suggests that the N-terminal region of the protein might bind to a second target more likely on the plasma membrane where IF_1 and CaM colocalize and where CaM is anchored to lipid rafts (*25*). Moreover, we can safely state that CaM and F1 can compete for the binding of IF_1 within the physiologic pH range. In fact, *in vitro* at pH 6.7 CaM prevents IF_1 from inhibiting both F1 (*2*, *4*) and F_OF_1ATPase (*2*) and that both IF_1−F1 and IF_1−CaM complexes have K_d in the nanomolar range (*2*, *38*). Noteworthy, selective increase in IF_1 expression on the cell surface that may evoke some specific regulation has been observed to occur and modulate cell surface−F_OF_1 activity in response to different stimuli, i.e., TNFα in HUVEC cells and acute cholestasis in rat liver (*27*, *39*). Thus, we suggest that CaM on the cell surface may sequester free IF_1 even in the presence of F_OF_1 and may modulate the amount of the inhibitory IF_1 in response to a proper stimulus (*25*).

SUPPORTING INFORMATION AVAILABLE

Example of the limited proteolysis experiments, showing the MALDI-MS analysis of the aliquots withdrawn following 0, 5, and 20 min of digestion with Glu-C endoprotease; and the SDS−PAGE analysis of the pull-down experiment carried out with biotinylated IF_1. This material is available free of charge via the Internet at http://pubs.acs.org.

REFERENCES

1. Cabezon, E., Runswick, M. J., Leslie, A. G. W., and Walker, J. E. (2001) The structure of bovine IF(1), the regulatory subunit of mitochondrial F-ATPase. *EMBO J. 20*, 6990–6996.
2. Contessi, S., Haraux, F., Mavelli, I., and Lippe, G. (2005) Identification of a conserved Calmodulin-binding motif in the sequence of F_OF_1ATPsynthase inibhitor protein. *J. Bioenerg. Biomembr. 37*, 317–326.
3. Cabezon, E., Butler, P. J., Runswick, M. J., and Walker, J. E. (2000) Modulation of the oligomerization state of the bovine F1-ATPase inhibitor protein, IF1, by pH. *J. Biol. Chem. 275*, 25460–25464.
4. Pedersen, P. L., and Hullihen, J. (1984) Inhibitor peptide of mitochondrial proton adenosine triphosphatase. Neutralization of its inhibitory action by calmodulin. *J. Biol. Chem. 259*, 15148–15153.
5. Schwerzmann, K., Muller, M., and Carafoli, E. (1985) The inhibitor peptide of the mitochondrial F1.F0-ATPase interacts with calmodulin and stimulates the calmodulin-dependent Ca2+-ATPase of erythrocytes. *Biochim. Biophys. Acta 816*, 63–67.
6. Strynadka, N. C., and James, M. N. (1989) Crystal structures of the helix-loop-helix calcium-binding proteins. *Annu. Rev. Biochem. 58*, 951–998.
7. Persechini, A., Moncrief, N. D., and Kretsinger, R. H. (1989) The EF-hand family of calcium-modulated proteins. *Trends Neurosci. 12*, 462–467.
8. Meador, W. E., Means, A. R., and Quiocho, F. A. (1993) Modulation of calmodulin plasticity in molecular recognition on the basis of x-ray structures. *Science 262*, 1718–1721.
9. Barbato, G., Ikura, M., Kay, L. E., Pastor, R. W., and Bax, A. (1992) Backbone dynamics of calmodulin studied by 15N relaxation using inverse detected two-dimensional NMR spectroscopy: the central helix is flexible. *Biochemistry 31*, 5269–5278.
10. Yamniuk, A. P., and Vogel, H. J. (2004) Calmodulin's flexibility allows for promiscuity in its interactions with target proteins and peptides. *Mol. Biotechnol. 27*, 33–57.
11. Ikura, M., and Ames, J. B. (2006) Genetic polymorphism and protein conformational plasticity in the calmodulin superfamily: two ways to promote multifunctionality. *Proc. Natl. Acad. Sci. U.S.A. 103*, 1159–1164.
12. Izumi, Y., Watanabe, H, Watanabe, N., Aoyama, A., Jinbo, Y., and Hayashi, N. (2008) Solution X-ray scattering reveals a novel structure of calmodulin complexed with a binding domain peptide from the HIV-1 matrix protein p17. *Biochemistry 47*, 7158–7166.
13. Yap, K. L., Kim, J., Truong, K., Sherman, M., Yuan, T., and Ikura, M. (2000) Calmodulin target database. *J. Struct. Funct. Genomics 1*, 8–14.
14. Popescu, S. C., Popescu, G. V., Bachan, S., Zhang, Z., Seay, M., Gerstein, M., Snyder, M., and Dinesh-Kumar, S. P. (2007) Differential binding of calmodulin-related proteins to their targets revealed through high-density Arabidopsis protein microarrays. *Proc. Natl. Acad. Sci. U.S.A. 104*, 4730–4735.
15. Bhattacharya, S., Bunick, C. G., and Chazin, W. J. (2004) Target selectivity in EF-hand calcium binding proteins. *Biochim. Biophys. Acta 1742*, 69–79.
16. Hoeflich, K. P., and Ikura, M. (2002) Calmodulin in action: diversity in target recognition and activation mechanisms. *Cell 108*, 739–742.
17. Schulz, D. M., Ihling, C., Clore, G. M., and Sinz, A. (2004) Mapping the topology and determination of a low-resolution three-dimensional structure of the calmodulin-melittin complex by chemical cross-linking and high-resolution FTICRMS: direct demonstration of multiple binding modes. *Biochemistry 43*, 4703–4715.
18. Ikura, M., Clore, G. M., Gronenborn, A. M., Zhu, G., Klee, C. B., and Bax, A. (1992) Solution structure of a calmodulin-target peptide complex by multidimensional NMR. *Science 256*, 632–638.
19. O'Neil, K. T., and DeGrado, W. F. (1990) How calmodulin binds its targets: sequence independent recognition of amphiphilic alpha-helices. *Trends Biochem. Sci. 15*, 59–64.
20. Vetter, S. W., and Leclerc, E. (2003) Novel aspects of calmodulin target recognition and activation. *Eur. J. Biochem. 270*, 404–414.

21. Osawa, M., Tokumitsu, H., Swindells, M. B., Kurihara, H., Orita, M., Shibanuma, T., Furuya, T., and Ikura, M. (1999) A novel target recognition revealed by calmodulin in complex with Ca2+-calmodulin-dependent kinase. *Nat. Struct. Biol. 6*, 819–824.
22. Elshorst, B., Hennig, M., Försterling, H., Diener, A., Maurer, M., Schulte, P., Schwalbe, H., Griesinger, C., Krebs, J., Schmid, H., Vorherr, T., and Carafoli, E. (1999) NMR solution structure of a complex of calmodulin with a binding peptide of the Ca^{2+} pump. *Biochemistry 38*, 12320–12332.
23. Schumacher, M. A., Rivard, A. F., Bachinger, H. P., and Adelman, J. P. (2001) Structure of the gating domain of a Ca^{2+}-activated K^+ channel complexed with Ca^{2+}/calmodulin. *Nature 410*, 1120–1124.
24. Drum, C. L., Yan, S. Z., Bard, J., Shen, Y. Q., Lu, D., Soelaiman, S., Grabarek, Z., Bohm, A., and Tang, W. J. (2002) Structural basis for the activation of anthrax adenylyl cyclase exotoxin by calmodulin. *Nature 415*, 396–402.
25. Contessi, S., Comelli, M., Cmet, S., Lippe, G., and Mavelli, I. (2007) IF(1) distribution in HepG2 cells in relation to ecto-F(0)F (1)ATP-synthase and calmodulin. *J. Bioenerg. Biomembr. 39*, 291–300.
26. Burwick, N. R., Wahl, M. L., Fang, J., Zhong, Z., Moser, T. L., Li, B., Capaldi, R. A., Kenan, D. J., and Pizzo, S. V. (2005) An Inhibitor of the F1 subunit of ATP synthase (IF1) modulates the activity of Angiostatin on the endothelial cell surface. *J. Biol. Chem. 280*, 1740–1745.
27. Giorgio, V., Bisetto, E., Franca, R., Harris, D. A., Passamonti, S., and Lippe, G. (2010) The ectopic F(O)F(1) ATP synthase of rat liver is modulated in acute cholestasis by the inhibitor protein IF1. *J. Bioenerg. Biomembr. 42*, 117–23.
28. van Raaij, M. J., Orriss, G. L., Montgomery, M. G., Runswick, M. J., Fearnley, I. M., Skehel, J. M., and Walker, J.E. (1996) The ATPase inhibitor protein from bovine heart mitochondria: the minimal inhibitory sequence. *Biochemistry 35*, 15618–15625.
29. Marino, G., Pucci, P., Birolo, L., and Ruoppolo, M. (2003) Exploitation of proteomic strategies in protein structure−function studies. *Pure Appl. Chem. 75*, 303–310.
30. Gordon-Smith, D. J., Carbajo, R. J., Yang, J. C., Videler, H., Runswick, M. J., Walker, J. E., and Neuhaus, D. (2001) Solution structure of a C-terminal coiled-coil domain from bovine IF_1: the inhibitor protein of F_1-ATPase. *J. Mol. Biol. 308*, 325–339.
31. Majava, V., Petoukhov, M. V., Hayashi, N., Pirilä, P., Svergun, D. I., and Kursula, P. (2008) Interaction between the C-terminal region of human myelin basic protein and calmodulin: analysis of complex formation and solution structure. *BMC Struct. Biol. 8*, 10.
32. Majava, V., and Kursula, P. (2009) Domain swapping and different oligomeric states for the complex between Calmodulin and the Calmodulin-binding domain of Calcineurin A. *PLoS One 4*, e5402.
33. Black, D. J., Tran, Q. K., and Persechini, A. (2004) Monitoring the total available calmodulin concentration in intact cells over the physiological range in free Ca2+. *Cell Calcium 35*, 415–425.
34. Rhoads, A. R., and Friedberg, F. (1997) Sequence motifs for calmodulin recognition. *FASEB J. 11*, 331–340.
35. Peersen, O. B., Madsen, T. S., and Falke, J. J. (1997) Intermolecular tuning of calmodulin by target peptides and proteins: differential effects on Ca^{2+} binding and implications for kinase activation. *Protein Sci. 6*, 794–807.
36. Brown, S. E., Martin, S. R., and Bayley, P. M. (1997) Kinetic control of the dissociation pathway of calmodulin-peptide complexes. *J. Biol. Chem. 272*, 3389–3397.
37. Mirzoeva, S., Weigand, S., Lukas, T. J., Shuvalova, L., Anderson, W. F., and Watterson, D. M. (1999) Analysis of the functional coupling between Calmodulin's calcium binding and peptide recognition properties. *Biochemistry 38*, 14117–14118.
38. Gomez-Fernandez, J. C., and Harris, D. A. (1978) A thermodynamic analysis of the interaction between the mitochondrial coupling adenosine triphosphatase and its naturally occurring inhibitor protein. *Biochem. J. 176*, 967–975.
39. Cortés-Hernández, P., Domínguez-Ramírez, L., Estrada-Bernal, A., Montes-Sánchez, D. G., Zentella-Dehesa, A., de Gómez-Puyou, M. T., Gómez-Puyou, A., and García, J. J. (2005) The inhibitor protein of the F1FO-ATP synthase is associated to the external surface of endothelial cells. *Biochem. Biophys. Res. Commun. 330*, 844–849.